

# CALET

Calorimetric  
Electron  
Telescope



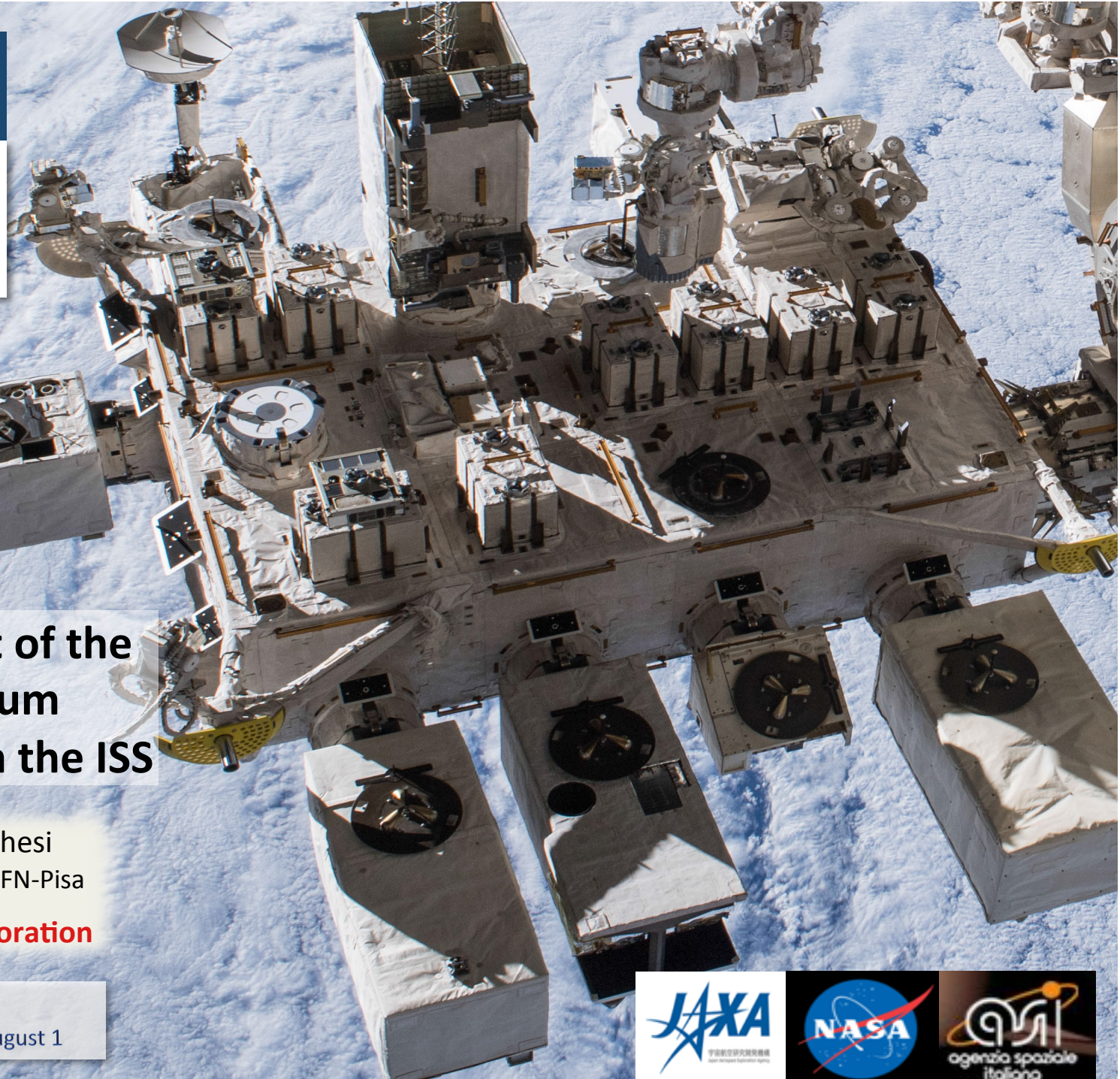
Measurement of the  
Proton Spectrum  
with CALET on the ISS

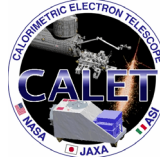
Pier Simone Marrocchesi  
University of Siena & INFN-Pisa

for the CALET Collaboration

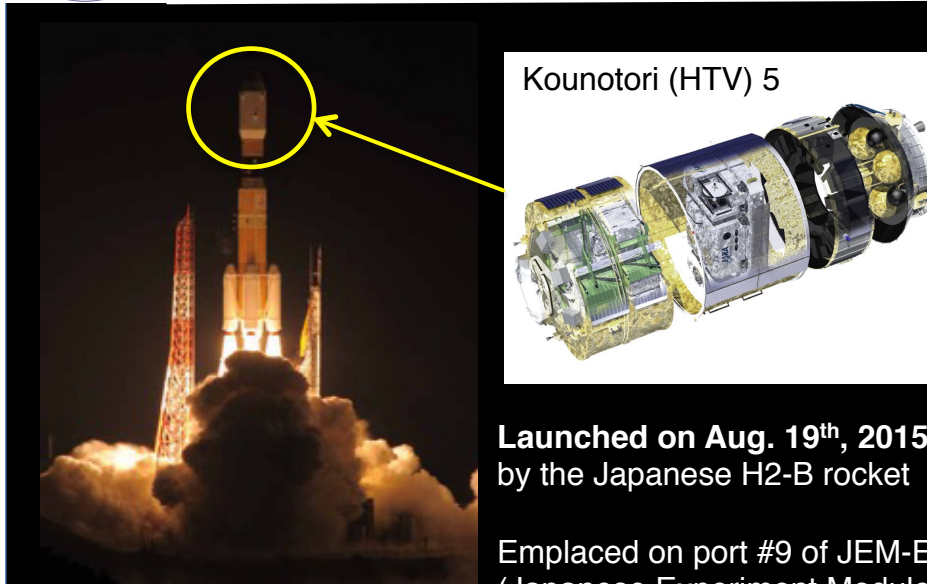
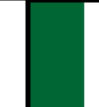
36th ICRC

Madison, 2019 July 24 – August 1





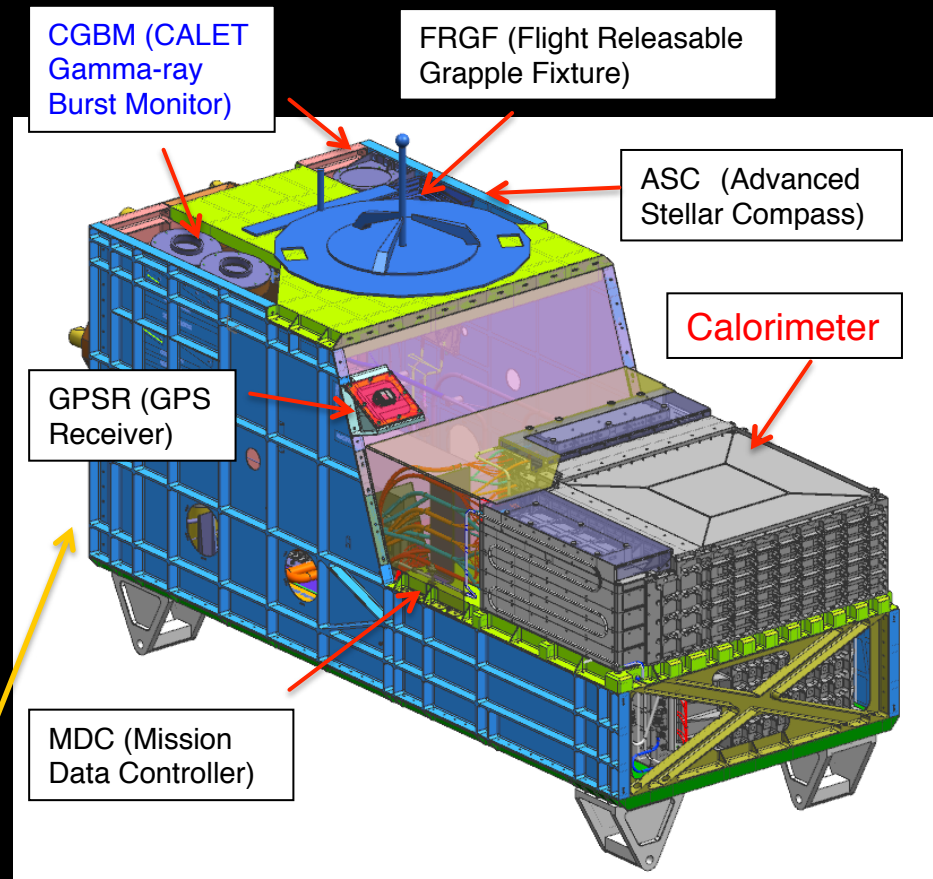
# CALET Payload



Launched on Aug. 19<sup>th</sup>, 2015  
by the Japanese H2-B rocket



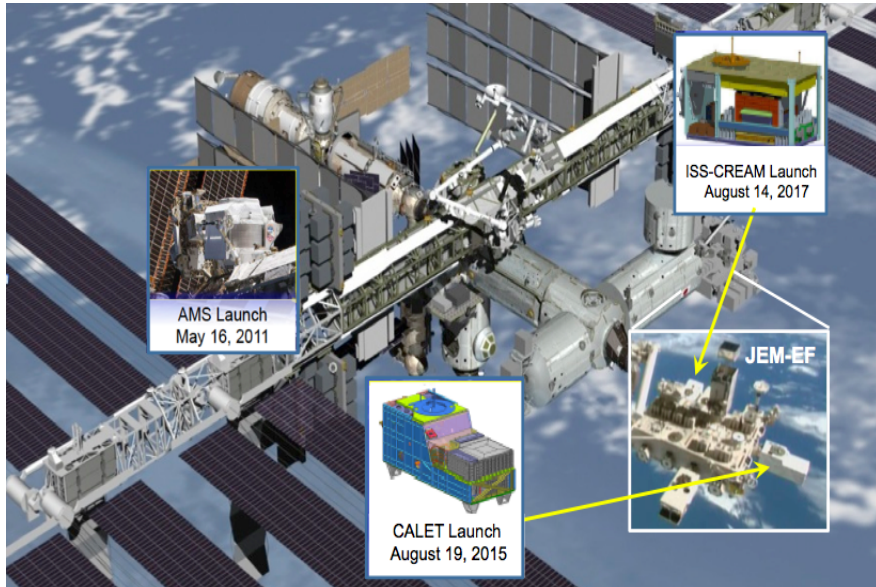
JEM/Port #9



- Mass: 612.8 kg JEM Standard Payload
- Size: 1850mm (L) × 800mm (W) × 1000mm (H)
- Power: 507 W (max)
- Telemetry: Medium 600 kbps (6.5GB/day)



# Cosmic Ray Observations aboard the ISS and CALET program



## Main CALET science objectives:

- ✧ **Electron observation** in 1 GeV - 20 TeV range.  
Design optimized for electron detection: high energy resolution and large e/p separation power + e.m. shower containment. Detailed study of spectral shape.  
**Search for Dark Matter and Nearby Sources**
- ✧ **Observation of cosmic-ray nuclei** in the energy region from 10 GeV to 1 PeV.  
**Unravelling the CR acceleration and propagation mechanism(s)**
- ✧ Detection of **transient phenomena** in space  
**Gamma-ray bursts, e.m. GW counterparts, Solar flares, Space Weather**

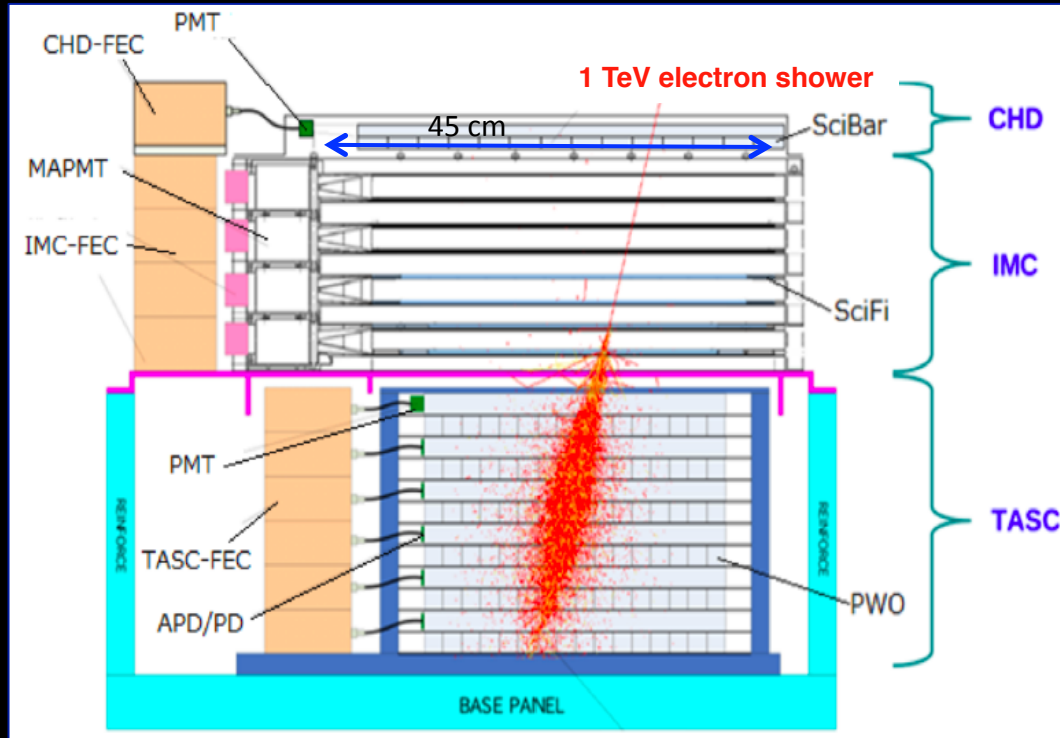
Scientific Objectives	Observation Targets	Energy Range
CR Origin and Acceleration	Electron spectrum Individual spectra of elements from proton to Fe Ultra Heavy Ions ( $26 < Z \leq 40$ ) Gamma-rays (Diffuse + Point sources)	1GeV - 20 TeV 10 GeV - 1000 TeV $> 600 \text{ MeV/n}$ 1 GeV - 1 TeV
Galactic CR Propagation	B/C and sub-Fe/Fe ratios	Up to some TeV/n
Nearby CR Sources	Electron spectrum	100 GeV - 20 TeV
Dark Matter	Signatures in electron/gamma-ray spectra	100 GeV - 20 TeV
Solar Physics	Electron flux (1GeV-10GeV)	$< 10 \text{ GeV}$
Gamma-ray Transients	Gamma-rays and X-rays	7 keV - 20 MeV



# CALET instrument in a nutshell

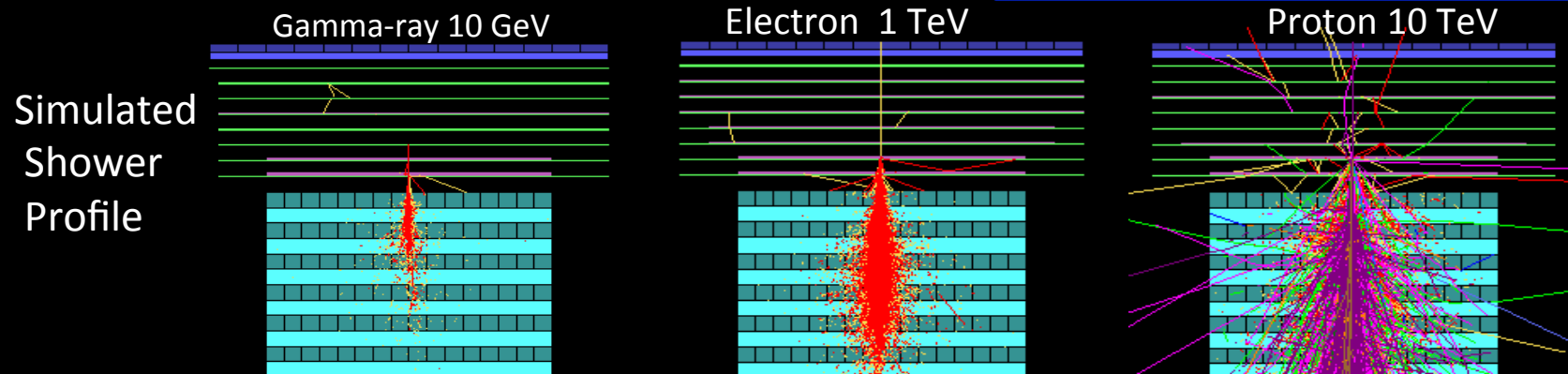
Field of view: ~ 45 degrees (from the zenith)

Geometrical Factor: ~ 1,040 cm<sup>2</sup>sr (for electrons)



## CALET: a unique set of key instruments

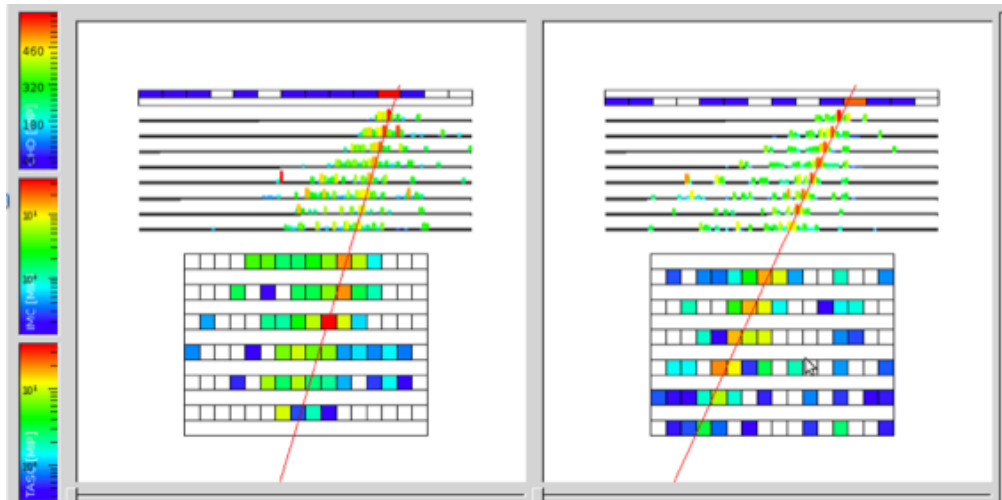
- CHD: a dedicated charge detector + multiple dE/dx sampling in the IMC allow the **identification of individual nuclear species** (charge resolution  $\sim 0.15\text{--}0.3$  e).
- IMC: high granularity (1mm) imaging pre-shower calorimeter to accurately reconstruct **the arrival direction** of incident particles ( $\sim 0.1^\circ$ ) and the **starting point** of electro-magnetic showers.  
SciFi + Tungsten absorbers:  $3 X_0$  ( $= 0.2 X_0 \times 5 + 1.0 X_0 \times 2$ )
- TASC: thick ( $27 X_0$ ) homogeneous PWO calorimeter allowing to extend electron measurements into the TeV energy region with  $\sim 2\%$  **energy resolution**.
- **Combined** ( $30 X_0, 1.2 \lambda_I$ ) they **separate electrons** from the abundant protons (rejection  $> 10^5$ ).



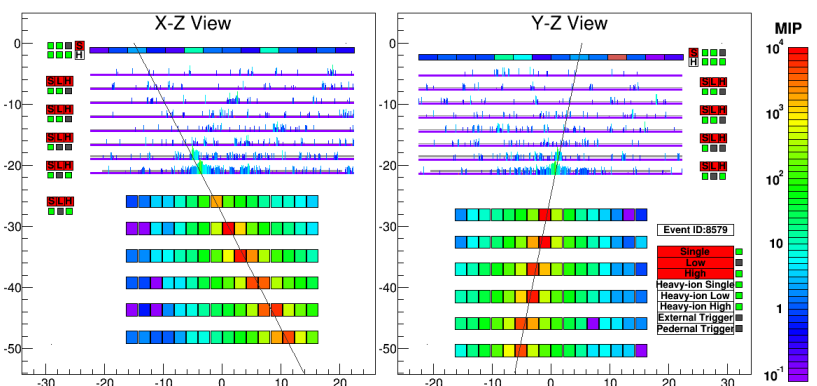


## Examples of Observed Events

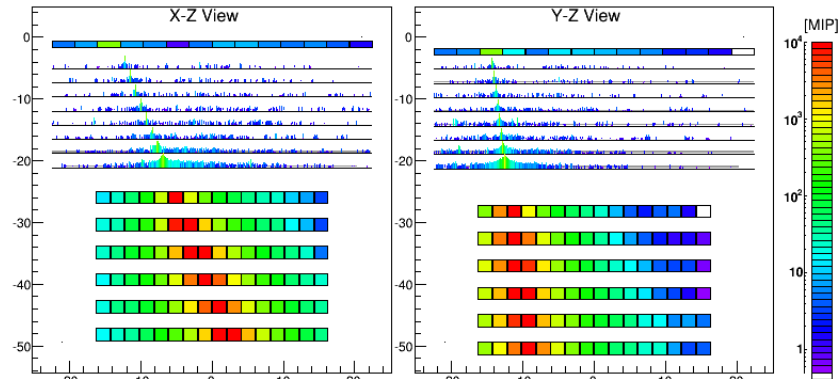
Multi-prong background event (interaction in CHD)



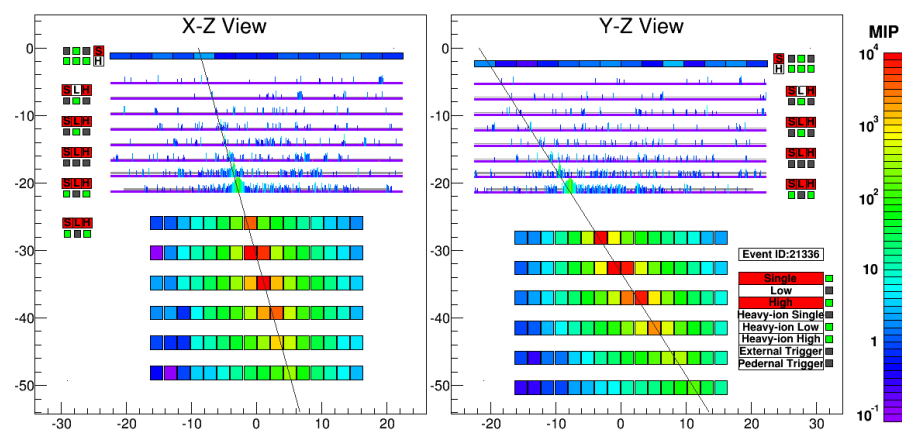
Proton,  $\Delta E=2.89$  TeV



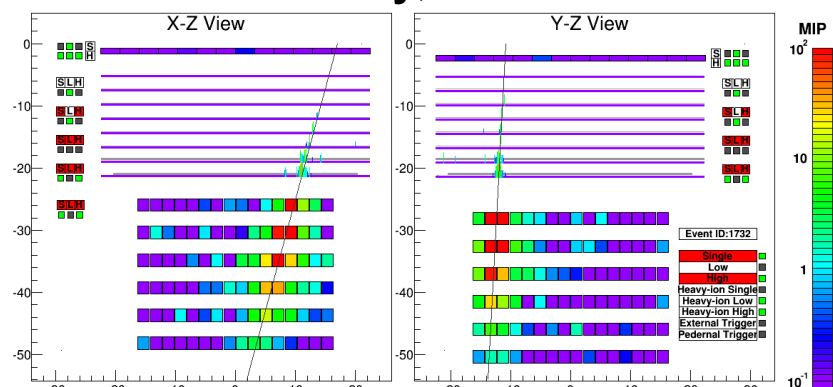
Iron,  $\Delta E=9.3$  TeV

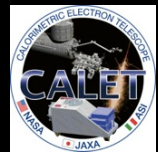


Electron,  $E=3.05$  TeV

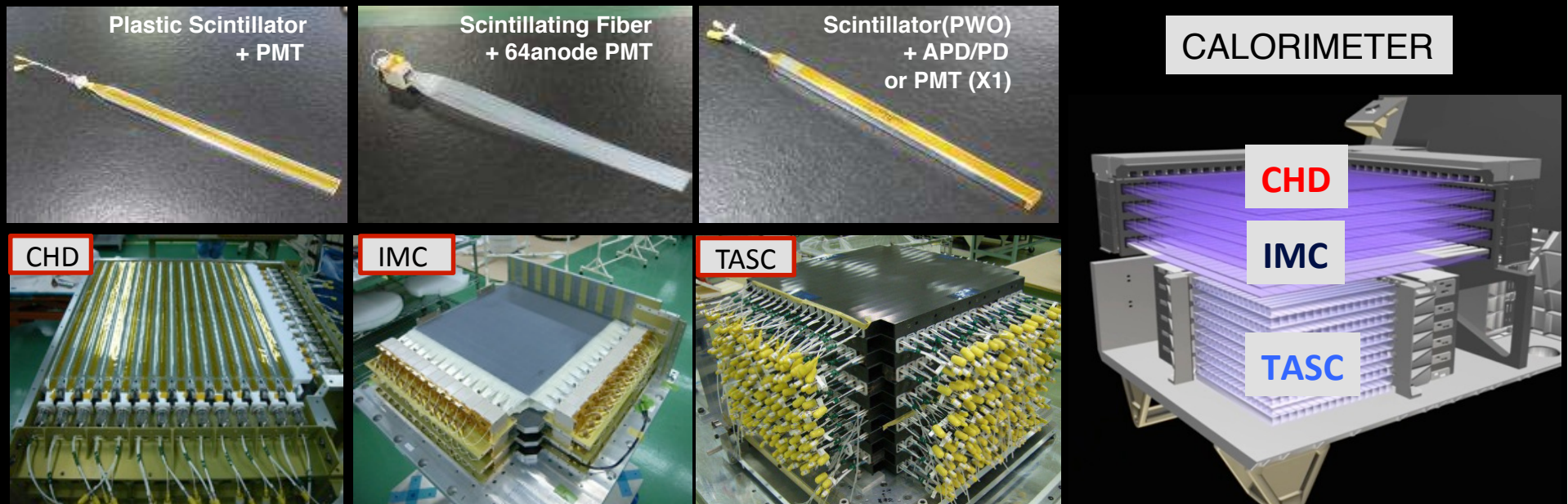


Gamma-ray,  $E=44.3$





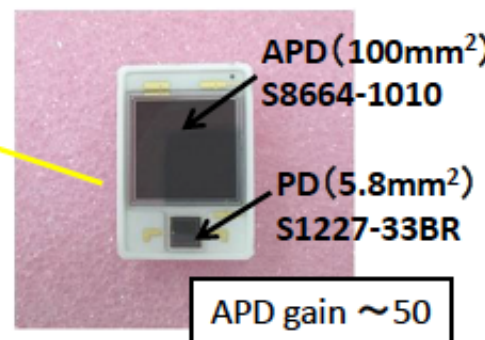
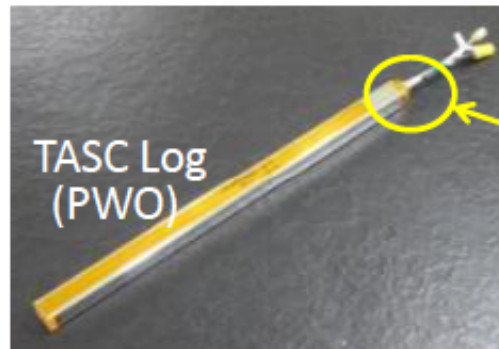
# CALET Instrument overview



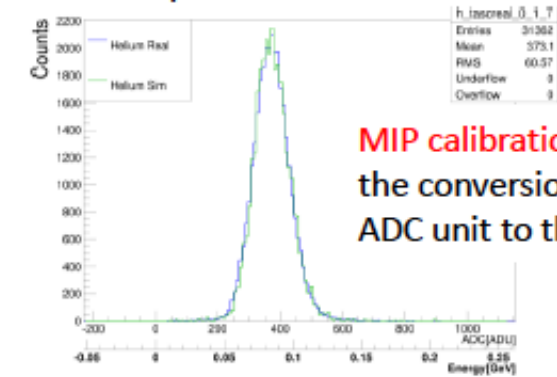
	<b>CHD</b> (Charge Detector)	<b>IMC</b> (Imaging Calorimeter)	<b>TASC</b> (Total Absorption Calorimeter)
<b>Measure</b>	<b>Charge (Z=1-40)</b>	<b>Tracking , Particle ID</b>	<b>Energy, e/p Separation</b>
<b>Geometry (Material)</b>	<b>Plastic Scintillators:</b> 28 paddles 14 paddles x 2 layers (X,Y) Paddle Size: $32 \times 10 \times 450 \text{ mm}^3$	<b>Scintillating Fibers:</b> 448 x 16 layers (X,Y) Scifi size: $1 \times 1 \times 448 \text{ mm}^3$ 7 Tungsten layers : $0.2X_0 \times 5 + 1X_0 \times 2$ Total Thickness: $3 X_0$	<b>PWO logs:</b> 16 x 12 layers (x,y): 192 logs log size: $19 \times 20 \times 326 \text{ mm}^3$ Total Thickness: $27 X_0$ , $\sim 1.2 \lambda_l$
<b>Readout</b>	<b>PMT+CSA</b>	<b>64-anode PMT+ ASIC</b>	<b>APD/PD+CSA</b> <b>PMT+CSA (for Trigger)@top layer</b>



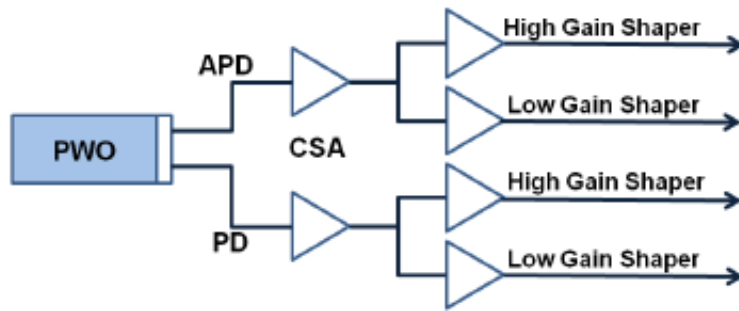
# Energy Measurement in a wide dynamic range 1-10<sup>6</sup> MIPs



"MIP" peak in PWO: Obs. vs. MC



MIP calibration determines the conversion factor from ADC unit to the energy

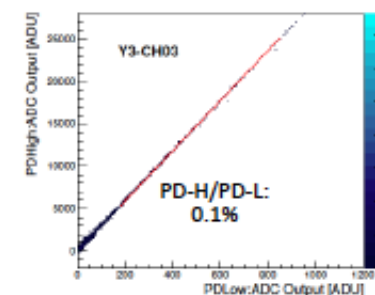
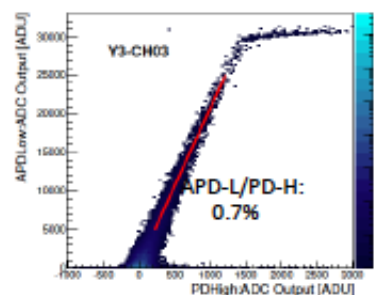
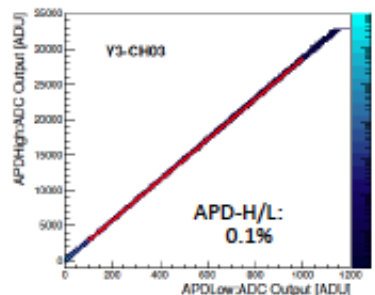


The whole dynamic range was calibrated by UV laser irradiation on ground :  
1) The linearity of each gain range is confirmed in the range of 1.4-2.5 %.  
2) Each channel covers from 1 MIP to 10<sup>6</sup> MIPs.

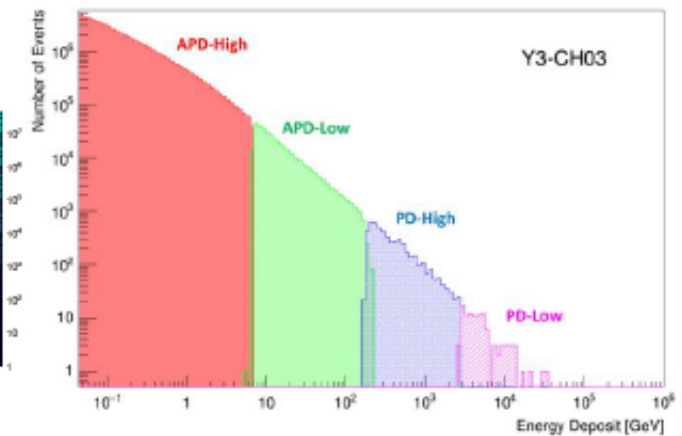
APD-H	APD-L	PD-H	PD-L
1.4%	1.5%	2.5%	2.2%

The correlation between adjacent gain ranges is calibrated by using in-flight data in each channel.

APD-H APD-L	APD-L PD-H	PD-H PD-L
0.1%	0.7%	0.1%



Example of energy distribution in one PWO log



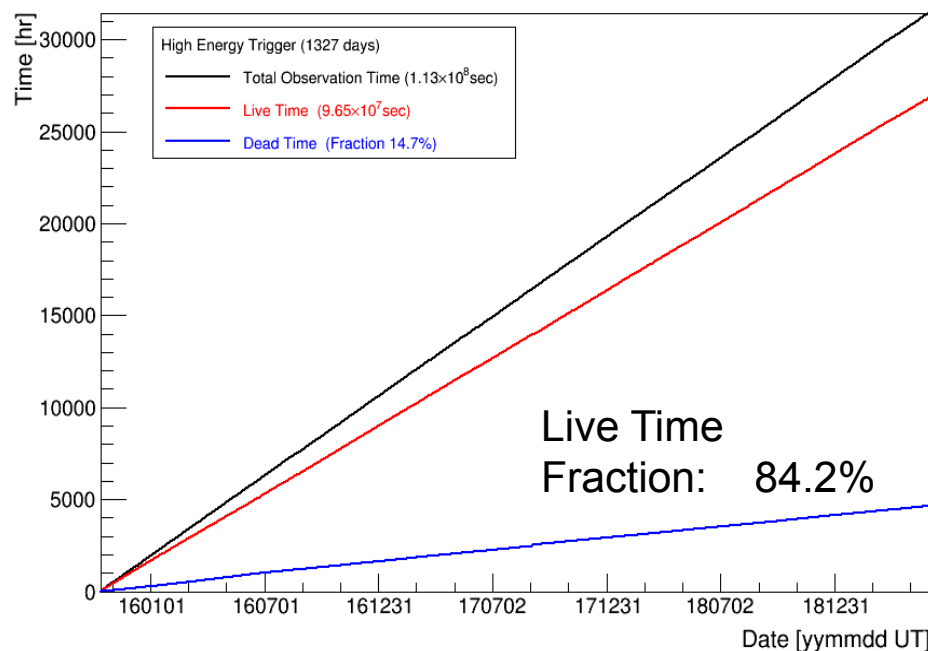


# Observations with High Energy Trigger (>10GeV)

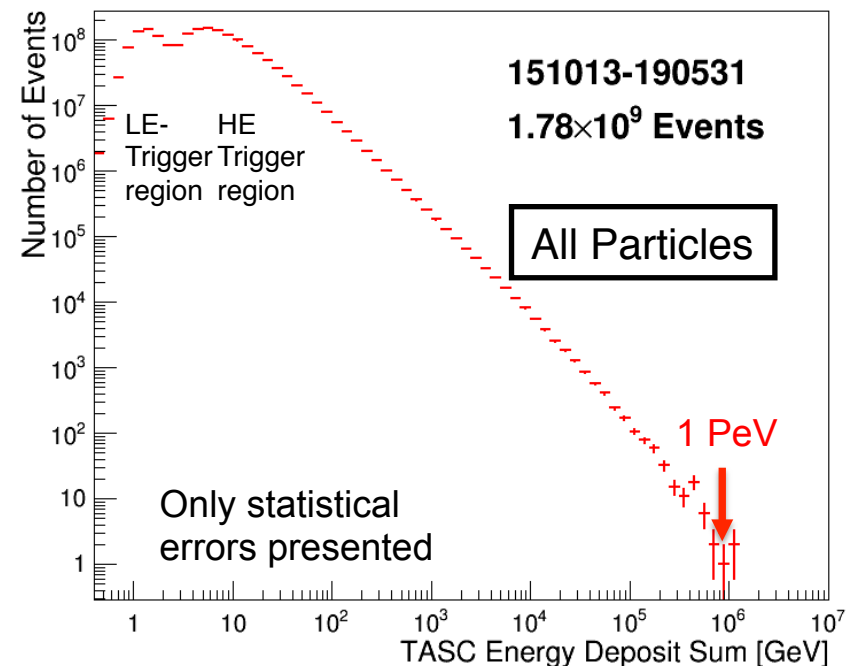
Observation with High Energy Trigger for 1327 days : Oct.13, 2015 – May 31, 2019

- The exposure, SQT, has reached  $\sim 116 \text{ m}^2 \text{ sr day}$  for electron observations under continuous and stable operations.
- Total number of triggered events is  $\sim 1.8 \text{ billion}$  with a live time fraction of  $\sim 84 \%$ .

Accumulated observation time (live, dead)



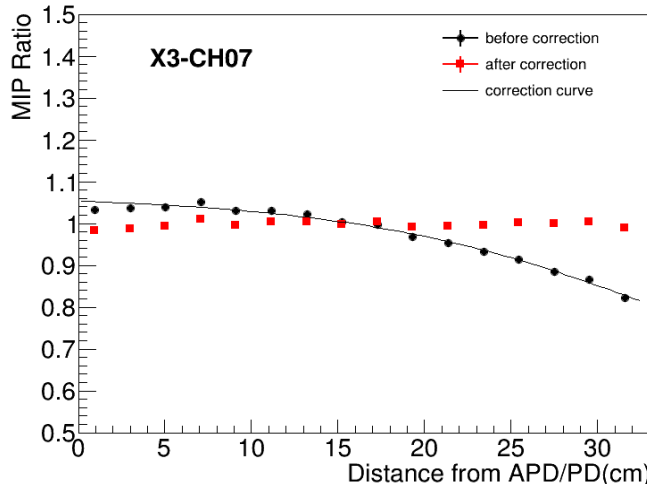
Distribution of deposit energies ( $\Delta E$ ) in TASC



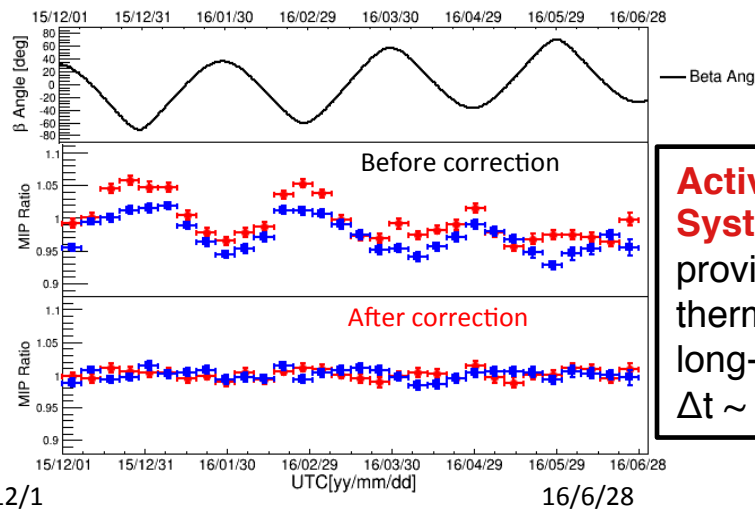


# Position and Temperature Calibration + Long-term Stability

Example of position dependence correction



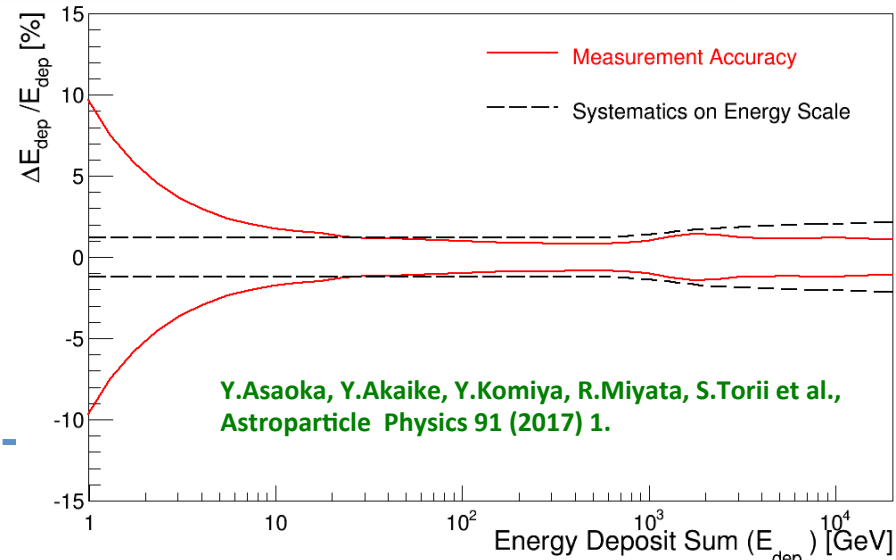
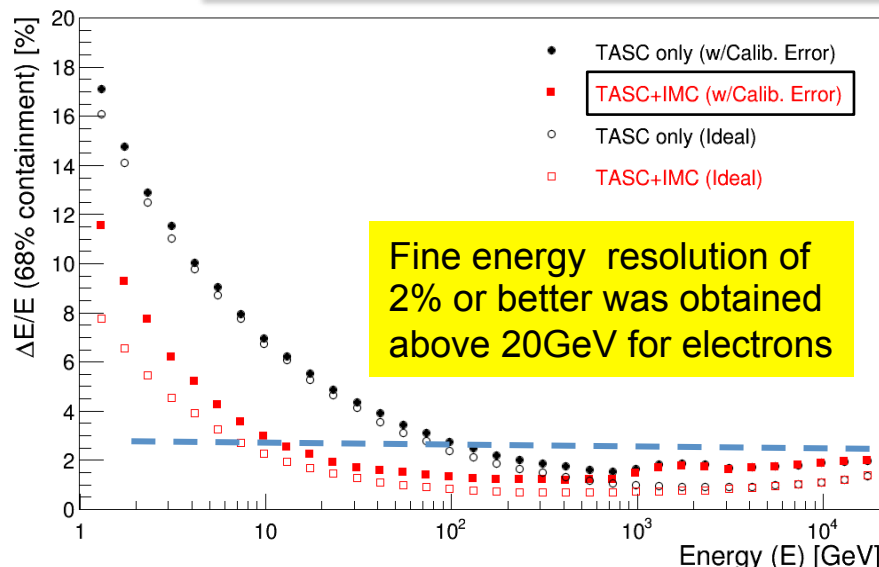
Examples of temperature change correction



TASC

**Active Thermal Control System (ATCS) on ISS**  
provides very stable thermal conditions during long-term observations:  
 $\Delta t \sim$  a few degrees

## Energy Resolution for Electrons by On-orbit Calibration

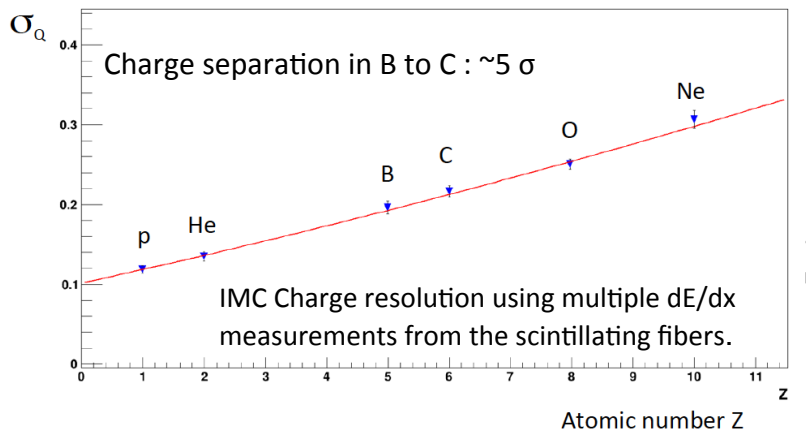
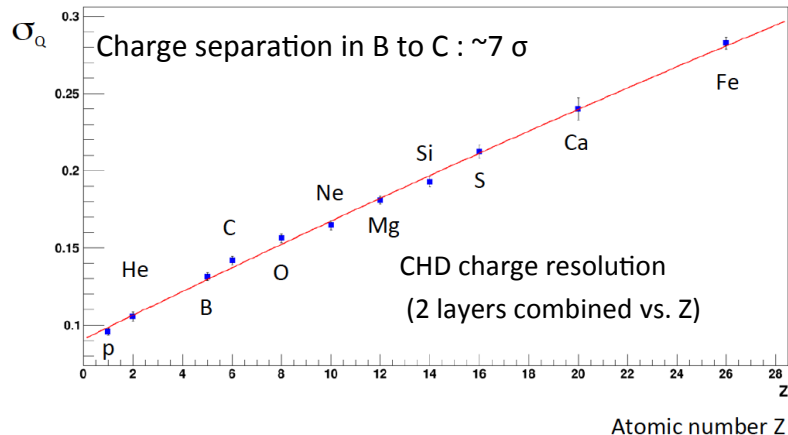


Y.Asaoka, Y.Akaike, Y.Komiya, R.Miyata, S.Torii et al.,  
Astroparticle Physics 91 (2017) 1.



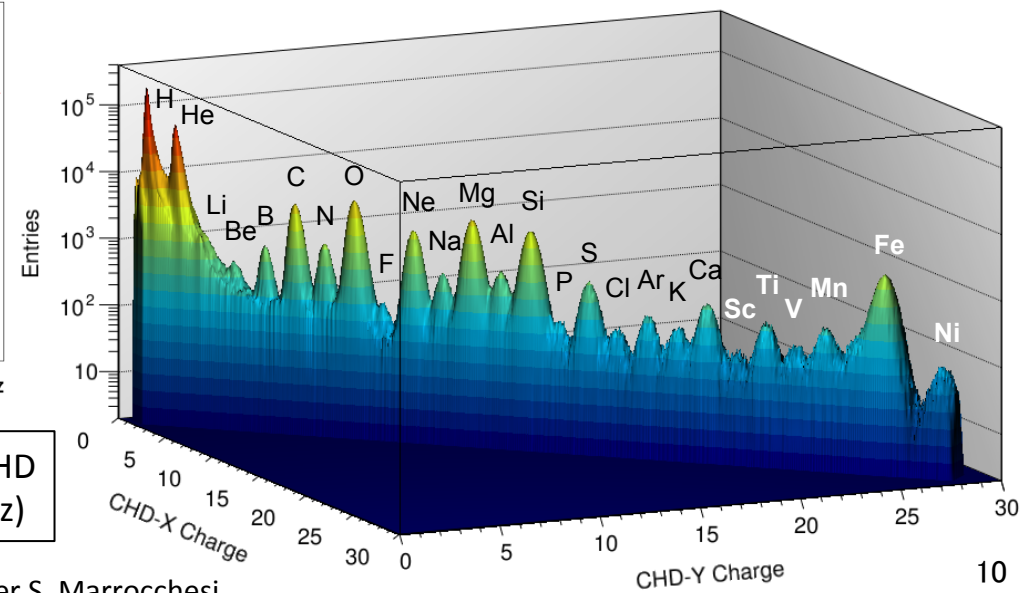
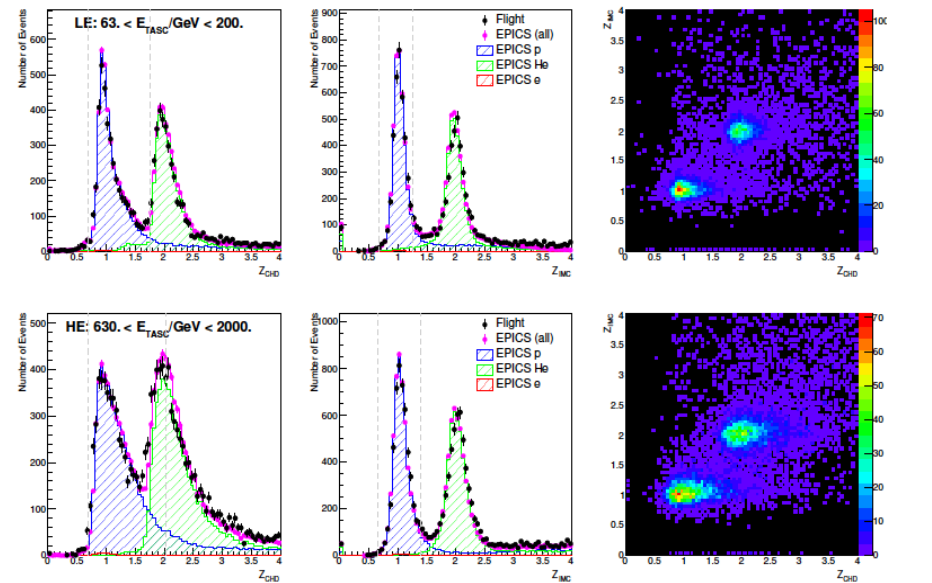
# Charge Identification of Nuclei with CHD and IMC

Single element selection for p, He and light nuclei is achieved by CHD+IMC charge analysis.



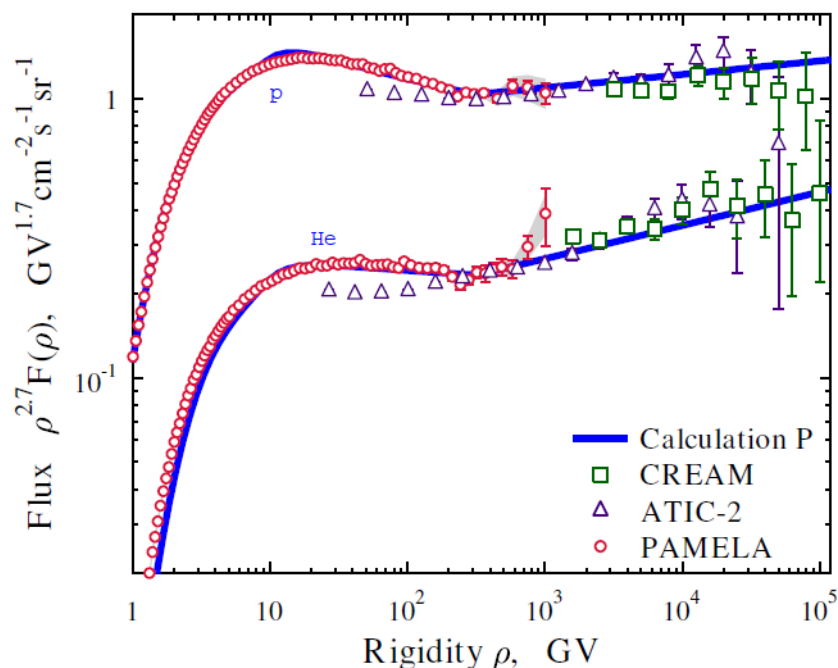
Deviation from  $Z^2$  response is corrected both in CHD and IMC using a core + halo ionization model (Voltz)

# Combined CHD-IMC proton-Helium charge-ID



# Direct measurements of proton and He spectra

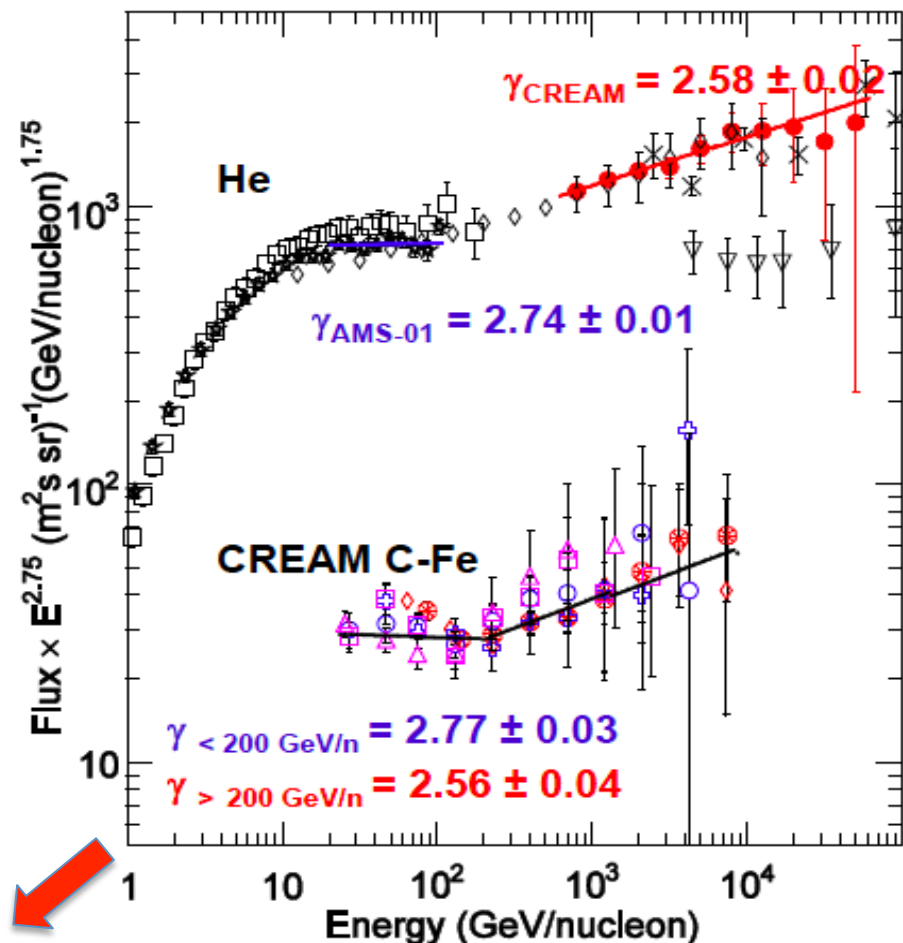
- PAMELA detected a spectral break in PROTON and HE spectra at  $R \sim 240$  GV



A single power-law seems inadequate to fit the spectra

The slope of  $Z>2$  NUCLEI at high energy looks similar to He and different from protons

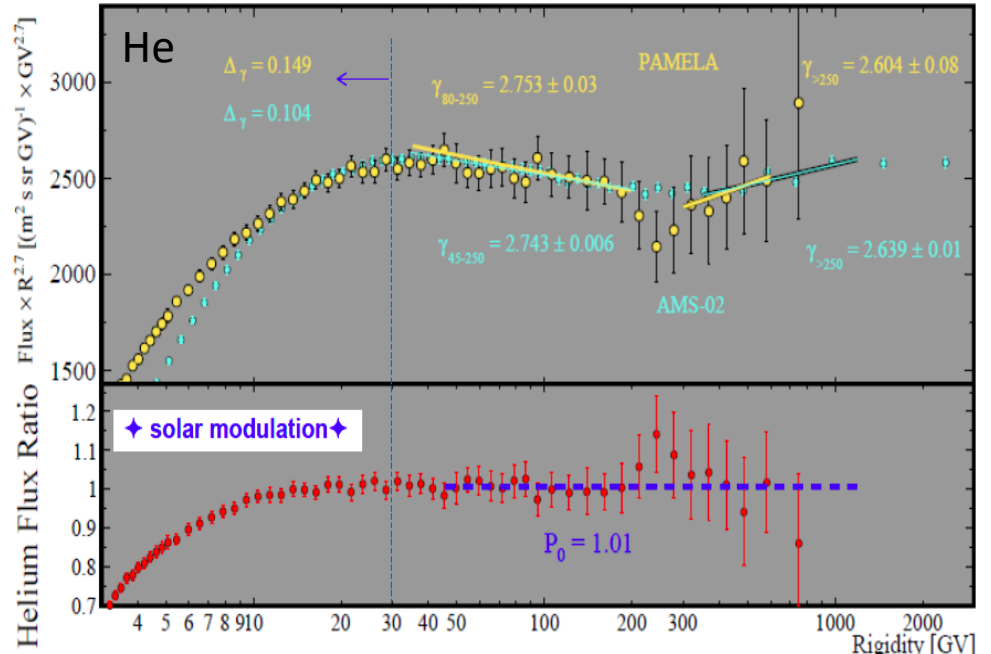
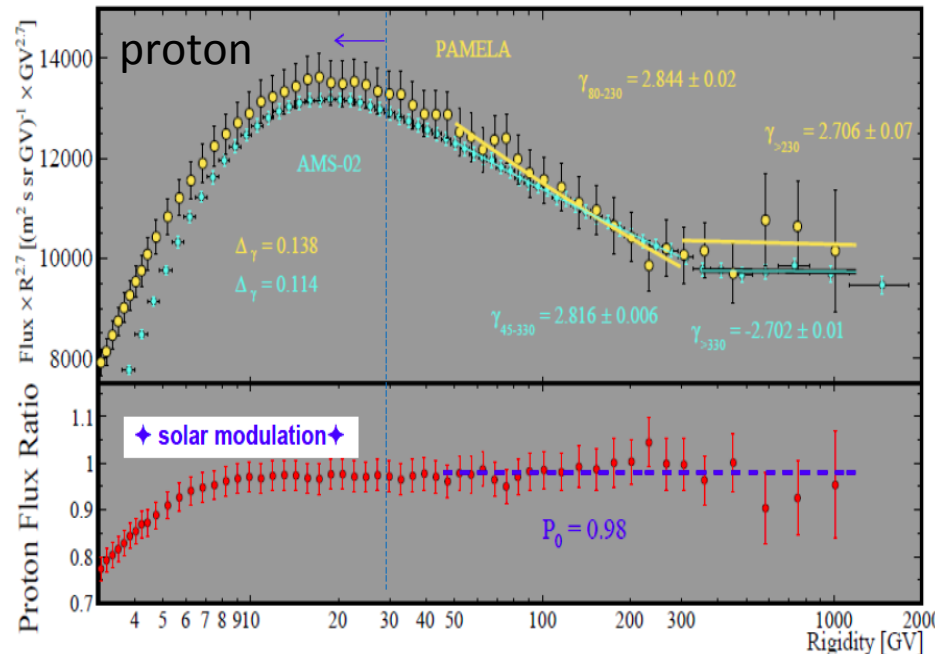
- The break also appears in the spectra of NUCLEI measured by CREAM (2010) up to several TeV/n



Ahn et al. ApJ 714, L89, 2010  
Yoon et al. ApJ 728, 122, 2011

# New era of precision spectral measurements:

- ❖ **p and He below 100 GeV:** % level agreement of magnetic spectrometers (BESS-TeV, PAMELA, AMS02)
- ❖ good agreement of PAMELA and AMS-02 on p and He spectra **below a few hundred GeV**



[M.Boezio @LNGS Jul 2016]

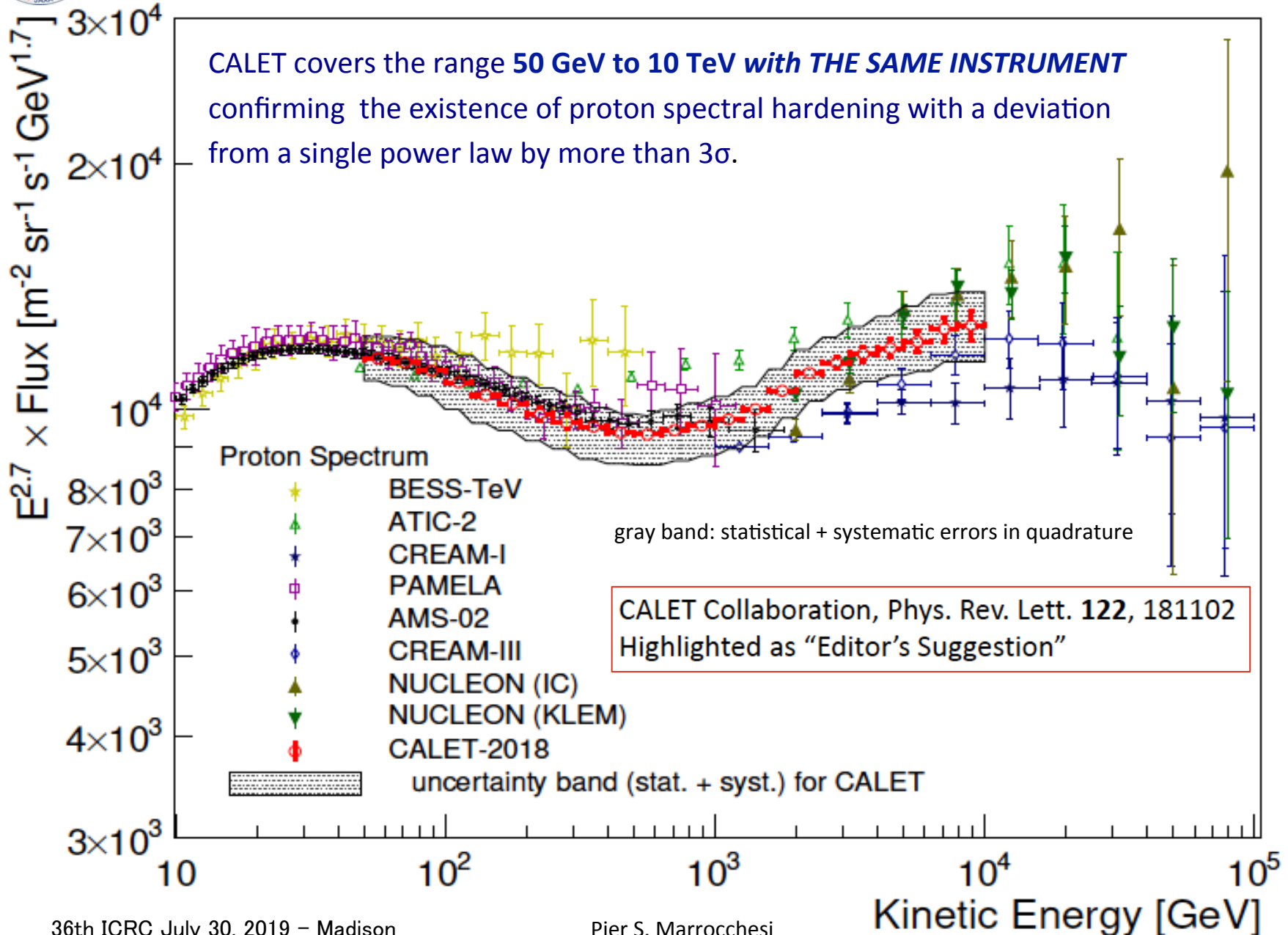
O. Adriani et al., Phys. Rep. 544 (2014) 323 ; M. Aguilar et al., PRL 114 (2015) 171103

O. Adriani et al., Science 332 (2011) 6025 ; M. Aguilar et al., PRL 115, (2015) 211101

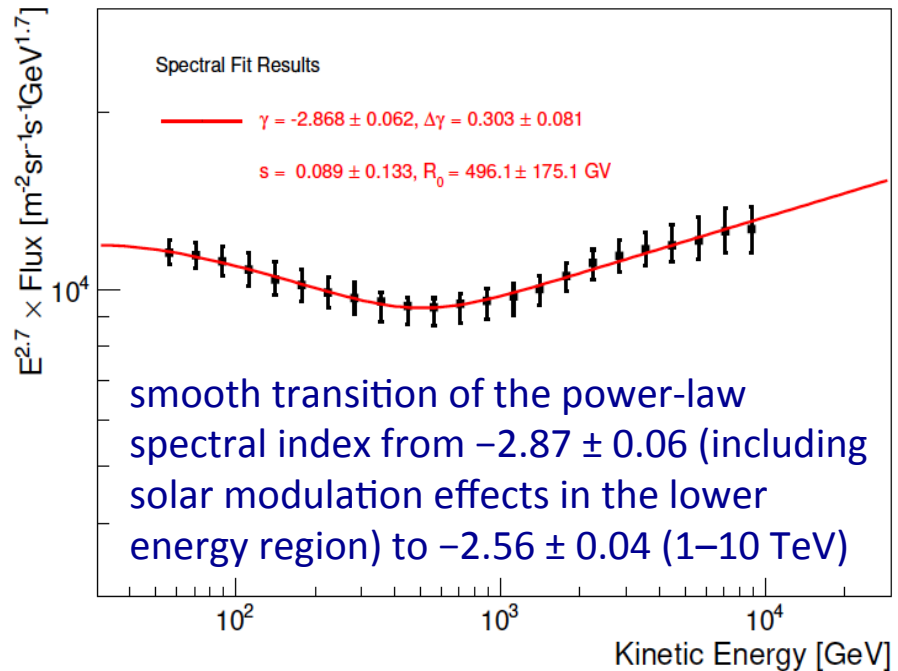
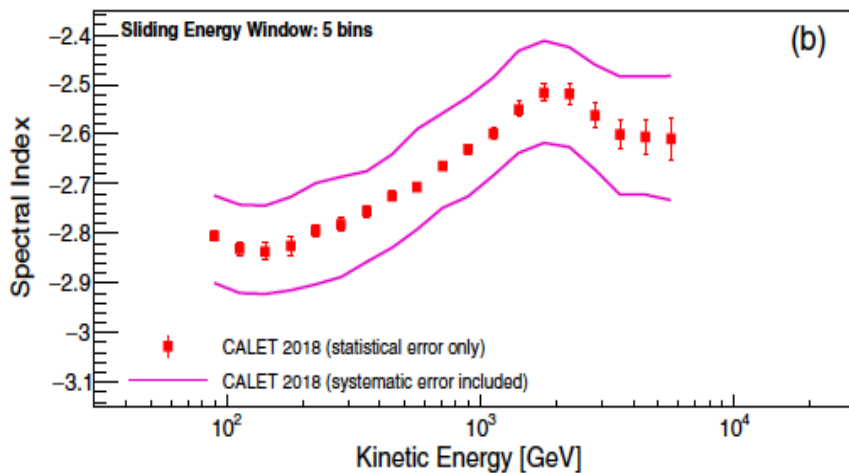
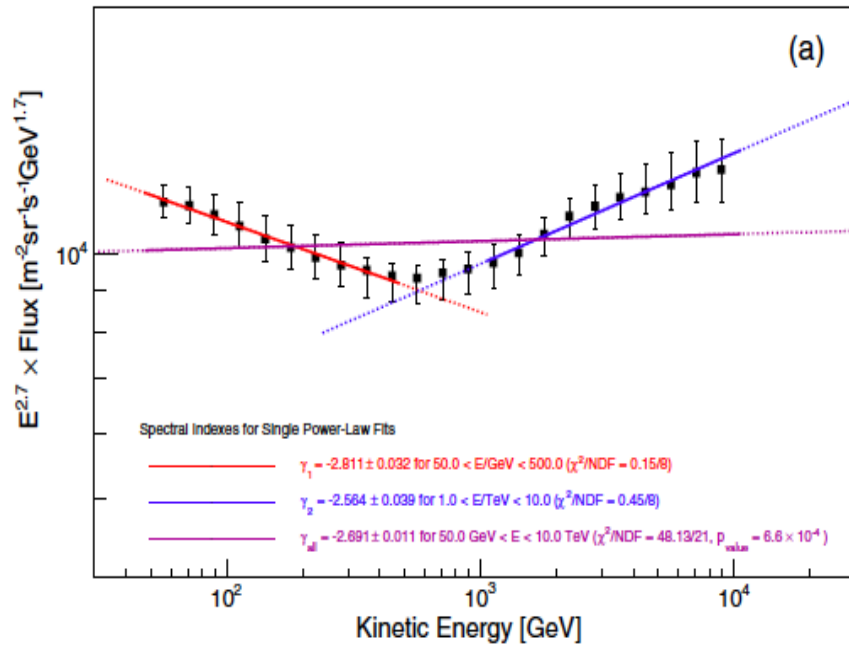
	fit range proton	$\gamma_p$	fit range He	$\gamma_{He}$
PAMELA	80-230 GV	-2.844±0.02	80-250 GV	-2.753±0.03
AMS-02	45-330 GV	-2.816±0.006	45-250 GV	-2.743±0.006



# Direct measurement of proton spectrum by CALET



# Spectral Behavior of Proton Flux



1. Subranges of 50–500GeV, 1–10TeV can be fitted with single power law function, but not the whole range (significance  $> 3\sigma$ ).
2. Progressive hardening up to the TeV region was observed.
3. “smoothly broken power-law fit” gives power law index consistent with AMS-02 in the low energy region, but shows larger index change and higher break energy than AMS-02.



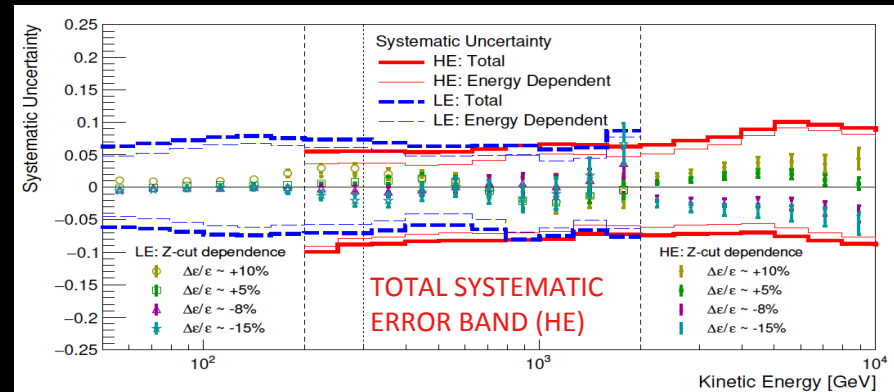
# Systematic Uncertainties (proton spectrum) Phys. Rev. Lett. 122, 181102 (2019)

- Study flux stability via scan of parameter space

## Energy independent (normalization)

- Live time
- Radiation environment
- Long-term stability
- Quality cuts

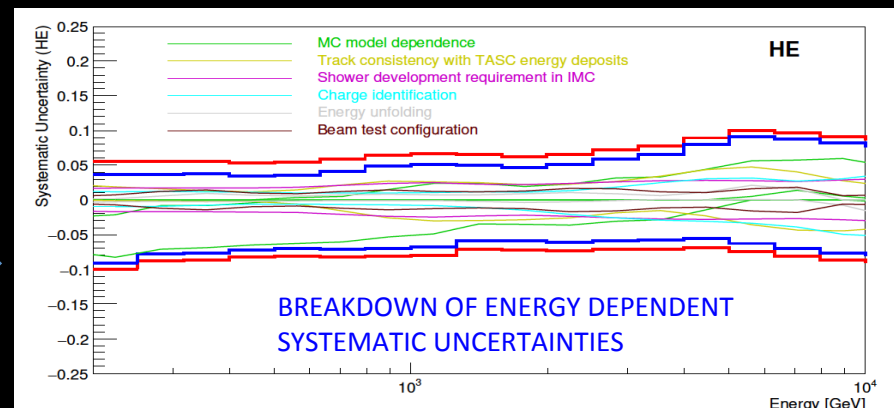
} 4.1%



## Energy dependent

- MC model dependence
- Track consistency with TASC energy deposits
- Shower development requirement in IMC
- Charge identification
- Energy unfolding
- Beam test related uncertainties

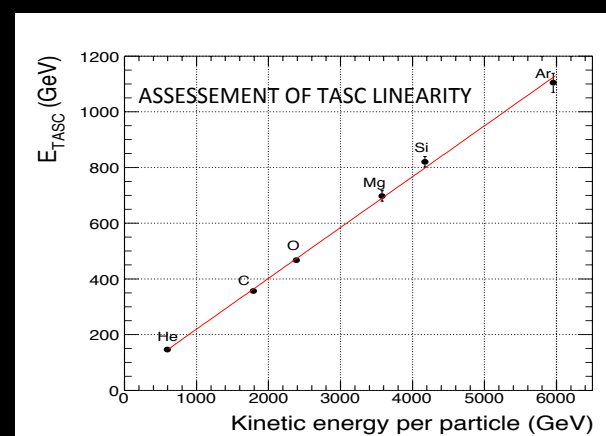
} →



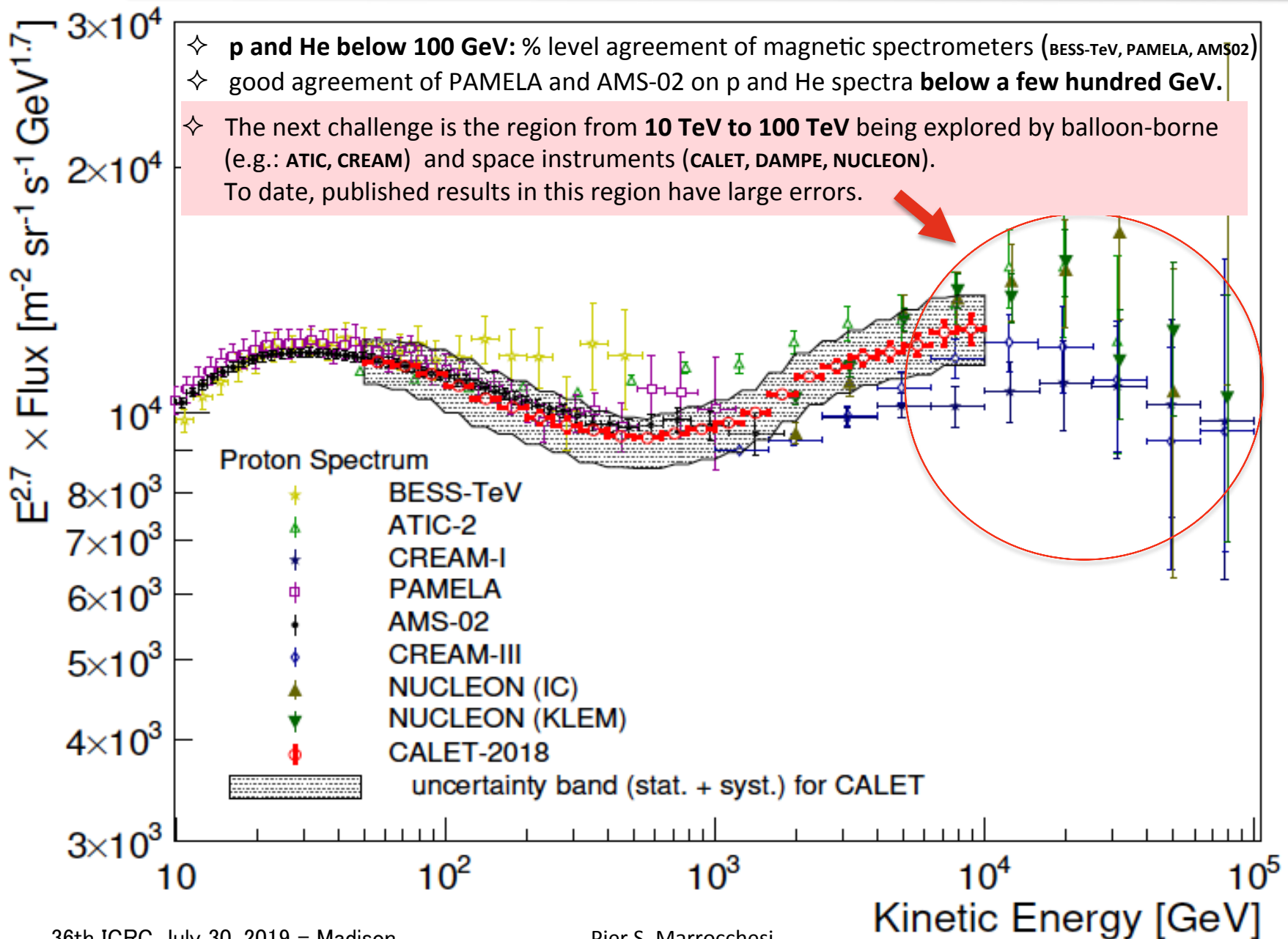
## Energy scale uncertainty

- beam test with < 400 GeV protons
- beam test with 150 GeV/n Ar fragments
- ground test with laser (response linearity)

} →



# Direct measurements of proton spectrum to date





# CALET: Summary and Future Prospects

- CALET was successfully launched on Aug. 19th, 2015. The observation campaign started on Oct. 13th, 2015. Excellent performance and remarkable stability of the instrument.
- As of May 31, 2019 total observation time is 1327 days with live time fraction to total time close to 84%. Nearly 1.8 billion events collected with low ( $> 1 \text{ GeV}$ ) + high energy ( $> 10 \text{ GeV}$ ) triggers.
- In-flight calibrations with p & He events + CERN beam tests with e, p and ion fragments. Linearity of energy measurements established up to  $10^6 \text{ MIP}$ .
- Measurement of electron+positron spectrum in 11 GeV - 4.8 TeV range using full acceptance Observation of a flux reduction above 1 TeV.
- Direct measurement of proton spectrum in 50 GeV – 10 TeV energy range. Spectral hardening observed above a few hundred GeV.
- Preliminary analysis of primary elements up to Fe and secondary-to-primary ratios.
- Preliminary analysis of UH cosmic rays up to Z=40.
- Study of diffuse and point sources with gamma-rays. Follow-up observations of GW events in X-ray and gamma-ray bands. CALET's CGBM detected 159 GRBs in the energy range 7 keV-20 MeV.
- After an initial period of 2 years CALET observation time has been extended to 5 years at least.



Thank you  
for your attention !



# CALET Collaboration Team



O. Adriani<sup>25</sup>, Y. Akaike<sup>2</sup>, K. Asano<sup>7</sup>, Y. Asaoka<sup>9,31</sup>, M.G. Bagliesi<sup>29</sup>, E. Berti<sup>25</sup>, G. Bigongiari<sup>29</sup>, W.R. Binns<sup>32</sup>, S. Bonechi<sup>29</sup>, M. Bongi<sup>25</sup>, P. Brogi<sup>29</sup>, A. Bruno<sup>15</sup>, J.H. Buckley<sup>32</sup>, N. Cannady<sup>13</sup>, G. Castellini<sup>25</sup>, C. Checchia<sup>26</sup>, M.L. Cherry<sup>13</sup>, G. Collazuol<sup>26</sup>, V. Di Felice<sup>28</sup>, K. Ebisawa<sup>8</sup>, H. Fukue<sup>8</sup>, T.G. Guzik<sup>13</sup>, T. Hams<sup>3</sup>, N. Hasebe<sup>31</sup>, K. Hibino<sup>10</sup>, M. Ichimura<sup>4</sup>, K. Ioka<sup>34</sup>, W. Ishizaki<sup>7</sup>, M.H. Israel<sup>32</sup>, K. Kasahara<sup>31</sup>, J. Kataoka<sup>31</sup>, R. Kataoka<sup>17</sup>, Y. Katayose<sup>33</sup>, C. Kato<sup>23</sup>, Y. Kawakubo<sup>1</sup>, N. Kawanaka<sup>30</sup>, K. Kohri<sup>12</sup>, H.S. Krawczynski<sup>32</sup>, J.F. Krizmanic<sup>2</sup>, T. Lomidze<sup>27</sup>, P. Maestro<sup>29</sup>, P.S. Marrocchesi<sup>29</sup>, A.M. Messineo<sup>27</sup>, J.W. Mitchell<sup>15</sup>, S. Miyake<sup>5</sup>, A.A. Moiseev<sup>3</sup>, K. Mori<sup>9,31</sup>, M. Mori<sup>21</sup>, N. Mori<sup>25</sup>, H.M. Motz<sup>31</sup>, K. Munakata<sup>23</sup>, H. Murakami<sup>31</sup>, S. Nakahira<sup>20</sup>, J. Nishimura<sup>8</sup>, G.A De Nolfo<sup>15</sup>, S. Okuno<sup>10</sup>, J.F. Ormes<sup>25</sup>, S. Ozawa<sup>31</sup>, L. Pacini<sup>25</sup>, F. Palma<sup>28</sup>, V. Pal'shin<sup>1</sup>, P. Papini<sup>25</sup>, A.V. Penacchioni<sup>29</sup>, B.F. Rauch<sup>32</sup>, S.B. Ricciarini<sup>25</sup>, K. Sakai<sup>3</sup>, T. Sakamoto<sup>1</sup>, M. Sasaki<sup>3</sup>, Y. Shimizu<sup>10</sup>, A. Shiomi<sup>18</sup>, R. Sparvoli<sup>28</sup>, P. Spillantini<sup>25</sup>, F. Stolzi<sup>29</sup>, S. Sugita<sup>1</sup>, J.E. Suh<sup>29</sup>, A. Sulaj<sup>29</sup>, I. Takahashi<sup>11</sup>, M. Takayanagi<sup>8</sup>, M. Takita<sup>7</sup>, T. Tamura<sup>10</sup>, N. Tateyama<sup>10</sup>, T. Terasawa<sup>7</sup>, H. Tomida<sup>8</sup>, S. Torii<sup>9,31</sup>, Y. Tunesada<sup>19</sup>, Y. Uchihori<sup>16</sup>, S. Ueno<sup>8</sup>, E. Vannuccini<sup>25</sup>, J.P. Wefel<sup>13</sup>, K. Yamaoka<sup>14</sup>, S. Yanagita<sup>6</sup>, A. Yoshida<sup>1</sup>, and K. Yoshida<sup>22</sup>

1) Aoyama Gakuin University, Japan

2) CRESST/NASA/GSFC and Universities Space Research Association, USA

3) CRESST/NASA/GSFC and University of Maryland, USA

4) Hirosaki University, Japan

5) Ibaraki National College of Technology, Japan

6) Ibaraki University, Japan

7) ICRR, University of Tokyo, Japan

8) ISAS/JAXA Japan

9) JAXA, Japan

10) Kanagawa University, Japan

11) Kavli IPMU, University of Tokyo, Japan

12) KEK, Japan

13) Louisiana State University, USA

14) Nagoya University, Japan

15) NASA/GSFC, USA

16) National Inst. of Radiological Sciences, Japan

17) National Institute of Polar Research, Japan

18) Nihon University, Japan

19) Osaka City University, Japan

20) RIKEN, Japan

21) Ritsumeikan University, Japan

22) Shibaura Institute of Technology, Japan

23) Shinshu University, Japan

24) University of Denver, USA

25) University of Florence, IFAC (CNR) and INFN, Italy

26) University of Padova and INFN, Italy

27) University of Pisa and INFN, Italy

28) University of Rome Tor Vergata and INFN, Italy

29) University of Siena and INFN, Italy

30) University of Tokyo, Japan

31) Waseda University, Japan

32) Washington University-St. Louis, USA

33) Yokohama National University, Japan

34) Yukawa Institute for Theoretical Physics, Kyoto University, Japan



# CALET Collaboration Team



O. Adriani<sup>25</sup>, Y. Akaike<sup>2</sup>, K. Asano<sup>7</sup>, Y. Asaoka<sup>9,31</sup>, M.G. Bagliesi<sup>29</sup>, E. Berti<sup>25</sup>, G. Bigongiari<sup>29</sup>, W.R. Binns<sup>32</sup>, S. Bonechi<sup>29</sup>, M. Bongi<sup>25</sup>, P. Brogi<sup>29</sup>, A. Bruno<sup>15</sup>, J.H. Buckley<sup>32</sup>, N. Cannady<sup>13</sup>, G. Castellini<sup>25</sup>, C. Checchia<sup>26</sup>, M.L. Cherry<sup>13</sup>, G. Collazuol<sup>26</sup>, V. Di Felice<sup>28</sup>, K. Ebisawa<sup>8</sup>, H. Fuke<sup>8</sup>, T.G. Guzik<sup>13</sup>, T. Hams<sup>3</sup>, N. Hasebe<sup>31</sup>, K. Hibino<sup>10</sup>, M. Ichimura<sup>4</sup>, K. Ioka<sup>34</sup>, W. Ishizaki<sup>7</sup>, M.H. Israel<sup>32</sup>, K. Kasahara<sup>31</sup>, J. Kataoka<sup>31</sup>, R. Kataoka<sup>17</sup>, Y. Katayose<sup>33</sup>, C. Kato<sup>23</sup>, Y. Kawakubo<sup>1</sup>, N. Kawanaka<sup>30</sup>, K. Kohri<sup>12</sup>, H.S. Krawczynski<sup>32</sup>, J.F. Krizmanic<sup>2</sup>, T. Lomidze<sup>27</sup>, P. Maestro<sup>29</sup>, P.S. Marrocchesi<sup>29</sup>, A.M. Messineo<sup>27</sup>, J.W. Mitchell<sup>15</sup>, S. Miyake<sup>5</sup>, A.A. Moiseev<sup>3</sup>, K. Mori<sup>9,31</sup>, M. Mori<sup>21</sup>, N. Mori<sup>25</sup>, H.M. Motz<sup>31</sup>, K. Munakata<sup>23</sup>, H. Murakami<sup>31</sup>, S. Nakahira<sup>20</sup>, J. Nishimura<sup>8</sup>, G.A. De Nolfo<sup>15</sup>, S. Okuno<sup>10</sup>, J.F. Ormes<sup>25</sup>, S. Ozawa<sup>31</sup>, L. Pacini<sup>25</sup>, F. Palma<sup>28</sup>, V. Pal'shin<sup>1</sup>, P. Papini<sup>25</sup>, A.V. Penacchioni<sup>29</sup>, B.F. Rauch<sup>32</sup>, S.B. Ricciarini<sup>25</sup>, K. Sakai<sup>3</sup>, T. Sakamoto<sup>1</sup>, M. Sasaki<sup>3</sup>, Y. Shimizu<sup>10</sup>, A. Shiomi<sup>18</sup>, R. Sparvoli<sup>28</sup>, P. Spillantini<sup>25</sup>, F. Stolzi<sup>29</sup>, S. Sugita<sup>1</sup>, J.E. Suh<sup>29</sup>, A. Sulaj<sup>29</sup>, I. Takahashi<sup>11</sup>, M. Takayanagi<sup>8</sup>, M. Takita<sup>7</sup>, T. Tamura<sup>10</sup>, N. Tateyama<sup>10</sup>, T. Terasawa<sup>7</sup>, H. Tomida<sup>8</sup>, S. Torii<sup>9,31</sup>, Y. Tunesada<sup>10</sup>, Y. Uchihori<sup>16</sup>, S. Ueno<sup>8</sup>, E. Vannuccini<sup>25</sup>, J.P. Wefel<sup>13</sup>, K. Yamaoka<sup>14</sup>, S. Yanagita<sup>6</sup>, A. Yoshida<sup>1</sup>, and K. Yoshida<sup>22</sup>





# Electron / Proton Discrimination

[Y.Asaoka, COSPAR 2108 E1.5-0023-18]

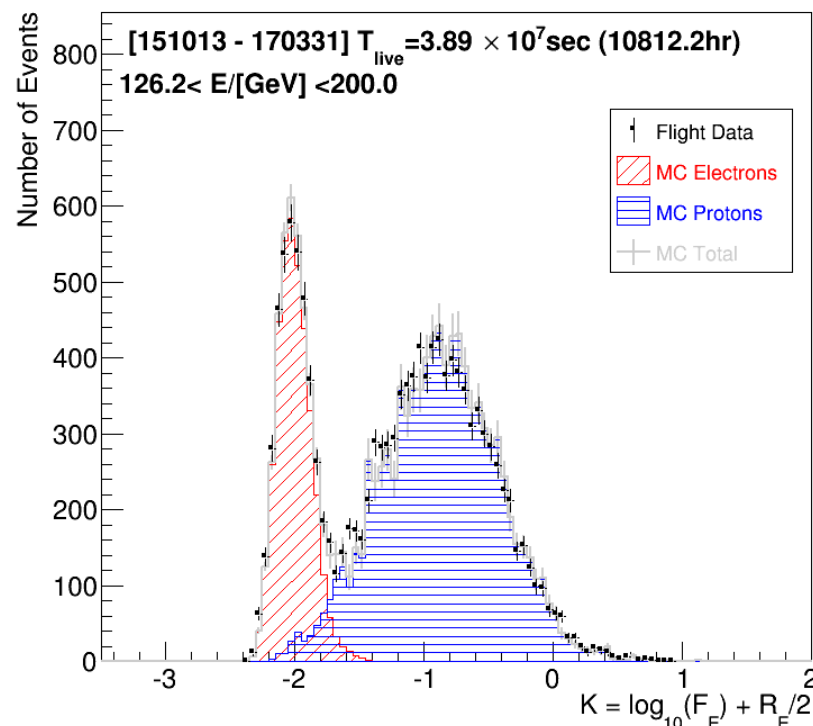
## Simple Two Parameter Cut

$F_E$ : Energy fraction of the bottom layer sum to the whole energy deposit sum in TASC

$R_E$ : Lateral spread of energy deposit in TASC-X1

Cut Parameter K is defined as follows:

$$K = \log_{10}(F_E) + 0.5 R_E / \text{cm}$$



## Boosted Decision Trees (BDT)

In addition to the two parameters on the left, TASC and IMC shower profile fits are used as discriminating variables

## BDT Response using 9 parameters

